Extended-State-Observer-Based Output Feedback Sliding Mode Control of Inertial Stabilized Platform

Jianliang Mao Jun Yang Qi Li Shihua Li
School of Automation, Southeast University, Nanjing 210096, China
Key Laboratory of Measurement and Control of CSE, Ministry of Education, Nanjing 210096, China
Email: j.yang84@seu.edu.cn

***Abstract*—Inertial stabilized platforms are extensively utilized to achieve high-precision pointing of optical axis in spite of vehicle motion or vibration. This paper develops an output feedback sliding mode control strategy for the inertial stabilized platform. The dynamic model taking into account various disturbed phenomena is established first. Not only the unknown state but also the lumped uncertainty is effectively estimated by extended state observer and brought into the sliding mode controller design. With the Lyapunov function technique, the tracking error of the inertial angular rate is verified to converge to an arbitrarily small region by adjusting certain control parameters. Furthermore, the switching gain is only required to be chosen to restrain the uncertainty caused by states estimation errors rather than disturbance itself, which substantially alleviates the chattering phenomenon. Comparative simulations are presented to show the effectiveness of the proposed method in two typical operation mode.**

***Index Terms*—Inertial stabilized platform, extended state observer, output feedback sliding mode control, uncertainty, chattering reduction**

I. Introduction

Inertial stabilized platforms (ISPs) are widely used in the optical-electronic tracking systems (OETSs) to keep the light of sight (LOS) free from the effects of vehicle motion or vibration [1]. The basic control task of the ISP is to achieve a high-precision pointing even in the presence of various disturbed phenomena, such as cross-couplings, mass unbalance, friction torque, parameter variations, and external wind-gust [2]. In order to make the LOS insensitive to the mentioned disturbances, two decoupled single-input-single-output (SISO) controllers with cascaded structure introduced in [2] are generally developed for the 2-degree-of-freedom (2-DOF) ISP system. In this strategy, for each gimbal, two PI controllers are designed to stabilize the inertial angular rate and the motor current, respectively. However, highly nonlinearity and heavy uncertainty complicate the application of the traditional PI control. Some advanced control methods, such as fuzzy control [3], $H\infty$ control [4], internal mode control [5] and neural network control [6] have been investigated to improve the control performance. Unfortunately, these feedback control approaches can only attenuate the time-varying disturbances to some extent rather than remove them as much as possible. In addition, in order to realize the controller design, at least three kinds of sensors are required for the signal measurements, i.e., fiber optical gyro (FOG) for the inertial angular rate measurement, optical encoder for the relative angle measurement, and hall sensor for the current measurement, which results in the growths of assembly difficulty and design cost.

How to counteract the adverse effects of nonvanishing uncertainties associating with an output feedback control strategy is imperative for ISP system. It is well known that sliding mode control (SMC) has provided an alternative way to deal with the model uncertainties and external disturbances. The key idea is to suppress the lumped uncertainty with switching function. Unfortunately, control chattering is unavoidable due to the fact that the switching gain is required to be designed larger than the boundary of disturbance [7]. Furthermore, it is only realizable for the case that all the system states are measurable. To this end, the unmeasurable states as well as the unknown disturbances should be estimated primarily.

The extended state observer (ESO) creatively put forward in Han's active disturbance rejection control (ADRC) structure [8] possesses the observation capability for both the states and the uncertainties. One of the greatest strengths of ADRC is that it is not dependent on the accurate mathematical model of the plant and the uniform boundedness can be guaranteed even in the presence of large dynamic uncertainties [9], [10]. However, the standard ESO is only available for a class of integral-chain systems [11], which can not be directly applied to the ISPs. Recently, some specific designs on the basis of the modified ESO are investigated for the hydraulic system [12], [13]. By virtue of the referred technique, it is feasible to design the ESO-based output feedback control for the ISPs.

In this paper, we propose a novel output feedback SMC strategy for 2-DOF ISP system. The control scheme taking into account multiple disturbances in the case of current and angle sensorless is considered. On the basis of the augmented state model of ISP, both the unknown state and the lumped uncertainty are effectively estimated by an ESO, which are later brought into the sliding mode controller design. With the Lyapunov function technique, the tracking error of angular rate is verified to converge to an arbitrarily small region by adjusting certain control parameters. Comparative simulations are presented to show the effectiveness of the proposed method.

II. Model Description

The detailed hardware structure of 2-DOF ISP system is shown in Fig. 1. A 2-axis FOG fixed on the inner gimbal (pitch-axis) is utilized to realize the stabilization on both pitch and yaw channels. Two permanent-magnet DC (PMDC)

978-1-5090-6161-7/17/$31.00

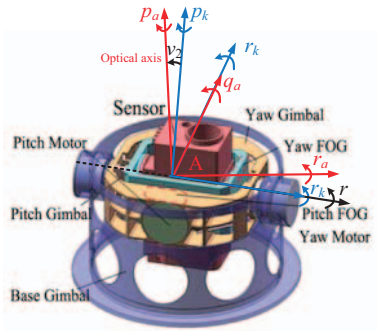

Fig. 1. Hardware structure of ISP system.

motors are applied here as the direct drive devices, due to their high torque when operating at a low speed.

For the angular rates of the base frame B, outer frame K, and inner frame A relative to inertial space, $\mathbf{\Omega_B}$, $\mathbf{\Omega_K}$, and $\mathbf{\Omega_A}$ are introduced, respectively, where $\mathbf{\Omega_B} = [p, q, r]^{\mathrm{T}}$, $\mathbf{\Omega_K} = [p_k, q_k, r_k]^{\mathrm{T}}$, and $\mathbf{\Omega_A} = [p_a, q_a, r_a]^{\mathrm{T}}$. The notations p, q, and r denote the roll, pitch, and yaw components of the inertial angular rate vector in frame B, respectively, and the analogous definitions are made for the other vectors. Let v_1 and v_2 denote the relative angles of yaw and pitch rotations. The dynamic model of the gimbal system can be derived as

$$J_i(v_2,t)\dot{\omega}_i = T_{ei} - F_c(\dot{\theta}_i,t) - T_i(\omega_i,v_2,t) - H_i(\omega_i,t) \quad (1)$$

where $i = q$ and r represent the pitch and yaw axes, respectively, $J_i(v_2,t)$ is the total moment of inertia imposed on the gimbal, ω_i is the inertial angular rate (i.e., $\omega_q = q_a, \omega_r = r_a$), T_{ei} represents the electromagnetic torque, $F_c(\dot{\theta}_i,t)$ represents the friction torque where θ_i is the relative angle (i.e., $\theta_r = v_1, \theta_q = v_2$), $T_i(\omega_i,v_2,t)$ represents the highly cross-coupling term, and $H_i(\omega_i,t)$ represents the unmodeled dynamics and external disturbances. For a detailed derivation, one can refer to [14].

In (1), the electromagnetic torque is generated by the PMDC motor, which is denoted as $T_{ei} = k_{ti}i_{ai}$, where k_{ti} is the torque coefficient and i_{ai} is the armature current. The friction torque can be divided into a linear part $B_i\dot{\theta}_i$ and a nonlinear part $F_i(\dot{\theta}_i,t)$ [10], where B_i is the viscous friction coefficient.

For the adopted PMDC motors, the voltage balance equation is presented as

$$L_{ai}\dot{i}_{ai} = V_iu_i - R_{ai}i_{ai} - k_{vi}\dot{\theta}_i \quad (2)$$

where L_{ai} is the armature inductance, V_i is the input DC voltage, u_i is the chopper duty cycle, R_{ai} is the armature resistance, and k_{vi} is the back-EMF coefficient.

Note that $\dot{\theta}_i$ commonly exists in (1) and (2), which can not be measured directly without an additional angle/velocity sensor. But it can be computed by using the expressions as follows:

$$\begin{aligned}\dot{\theta}_q &= \dot{v}_2 = \omega_q - \Omega_q(\omega_q,v_2,t),\\ \dot{\theta}_r &= \dot{v}_1 = \omega_r - \Omega_r(\omega_r,v_2,t)\end{aligned} \quad (3)$$

where $\Omega_q(\omega_q,v_2,t) = q_k$ and $\Omega_r(\omega_r,v_2,t) = r_a - r_a\sec v_2 + p_k\tan v_2$, denoting the structured uncertainties. By submitting (3) into (1) and (2), we can obtain the second-order dynamic model as

$$\begin{aligned}\dot{\omega}_i &= -\frac{B_i}{J_{oi}}\omega_i + \frac{k_{ti}}{J_{oi}}i_{ai} + \frac{D_{1i}}{J_{oi}},\\ \dot{i}_{ai} &= -\frac{k_{vi}}{L_{ai}}\omega_i - \frac{R_{ai}}{L_{ai}}i_{ai} + \frac{V_i}{L_{ai}}u_i + \frac{D_{2i}}{L_{ai}}\end{aligned} \quad (4)$$

where J_{oi} denotes the nominal value of $J_i(v_2,t)$ (i.e., $J_{oq} = J_{ay}, J_{or} = J_{az} + J_{kz}$ [14]), D_{1i} and D_{2i} represent the unmatched and matched lumped uncertainties, respectively, defined by

$$\begin{aligned}D_{1i} =& B_i\Omega_i(\omega_i,v_2,t) - F_i(\dot{\theta}_i,t) - T_i(\omega_i,v_2,t)\\ &- H_i(\omega_i,t) + d_{1i}(\omega_i,t),\\ D_{2i} =& k_{vi}\Omega_i(\omega_i,v_2,t) + d_{2i}(\omega_i,t)\end{aligned} \quad (5)$$

where $d_{1i}(\omega_i,t)$ and $d_{2i}(\omega_i,t)$ denote the parametric uncertainties caused by parameter variations of $J_i(v_2,t)$, B_i, k_{ti}, L_{ai}, V_i, R_{ai}, and k_{vi}. Note that the unmatched lumped uncertainty D_{1i} is composed of cross-couplings, friction torque, parameter variations, and external disturbances, which has the negative impact on the control accuracy of LOS. Consequently, it is imperative to counteract the influences of various disturbed phenomena for the high-precision control.

In this paper, we consider the case that only the inertial angular rates q_a and r_a are available. That is, in addition to the FOG, there are no additional sensors. By introducing a new state vector $[x_{1i}, x_{2i}]^{\mathrm{T}}$, where

$$\begin{aligned}x_{1i} =& \omega_i^* - \omega_i,\\ x_{2i} =& \dot{\omega}_i^* + \frac{B_i}{J_{oi}}\omega_i - \frac{k_{ti}}{J_{oi}}i_{ai} - \frac{D_{1i}}{J_{oi}},\end{aligned} \quad (6)$$

and ω_i^* is the desired angular rate which is preseted by the outer image tracker. System (4) can be rewritten as

$$\begin{aligned}\dot{x}_{1i} =& x_{2i},\\ \dot{x}_{2i} =& F_{ri}(x_{1i},x_{2i}) + b_iu_i + D_{di}\end{aligned} \quad (7)$$

where

$$\begin{aligned}&F_{ri}(x_{1i},x_{2i}) = \ddot{\omega}_i^* + F_{2i}(\dot{\omega}_i^* - x_{2i}) + F_{1i}(\omega_i^* - x_{1i}),\\ &D_{di} = -\frac{R_{ai}}{J_{oi}L_{ai}}D_{1i} - \frac{k_{ti}}{J_{oi}L_{ai}}D_{2i} - \frac{1}{J_{oi}}\dot{D}_{1i},\\ &F_{1i} = \frac{k_{ti}k_{vi} + R_{ai}B_i}{J_{oi}L_{ai}}, F_{2i} = \frac{B_i}{J_{oi}} + \frac{R_{ai}}{L_{ai}}, b_i = -\frac{k_{ti}V_i}{J_{oi}L_{ai}}.\end{aligned}$$

III. Controller Design

It is well known that the control frame of ISP is typically composed of stabilized loop and current loop [2]. To improve the dynamic response and disturbance rejection ability of the ISP, in this paper, the controller design of the inertial angular rate feedback loop is mainly investigated and the current loop is omitted since the signal is assumed to be unmeasurable. That is, the control task is to achieve a fast and accurate tracking performance of the inertial angular rate in the presence of various disturbed phenomena on the basis of system (7).

Before the controller design, the following assumption is made firstly.

Assumption 1: The derivative of uncertainty D_{di} is existing and bounded by a constant value L_i.

In this section, we will design an output feedback controller based on ESO and SMC method.

A. ESO Design

Extend the lumped disturbance D_{di} as an additional state, i.e., define $x_{3i} = D_{di}$. Let $\dot{D}_{di} = h_i$. The original plant in (7) can be rewritten as

$$\begin{aligned} \dot{\mathbf{x}}_\mathbf{i} &= \mathbf{A_i}\mathbf{x_i} + \mathbf{F_i}(\mathbf{x_i}) + \mathbf{B_i}b_i u_i + \mathbf{\Delta_i}, \\ y_i &= \mathbf{C_i}\mathbf{x_i} \end{aligned} \tag{8}$$

where

$$\begin{aligned} \mathbf{x_i} &= [x_{1i} \quad x_{2i} \quad x_{3i}]^{\mathrm{T}}, \mathbf{A_i} = \begin{bmatrix} 0 & 1 & 0 \\ 0 & 0 & 1 \\ 0 & 0 & 0 \end{bmatrix}, \\ \mathbf{F_i}(\mathbf{x_i}) &= [0 \quad F_{ri}(x_{1i}, x_{2i}) \quad 0]^{\mathrm{T}}, \mathbf{B_i} = [0 \quad 1 \quad 0]^{\mathrm{T}}, \\ \mathbf{\Delta_i} &= [0 \quad 0 \quad h_i]^{\mathrm{T}}, \mathbf{C_i} = [1 \quad 0 \quad 0]. \end{aligned}$$

For the augmented system (8), the ESO with linear type can be constructed as

$$\dot{\hat{\mathbf{x}}}_\mathbf{i} = \mathbf{A_i}\hat{\mathbf{x}}_\mathbf{i} + \mathbf{F_i}(\hat{\mathbf{x}}_\mathbf{i}) + \mathbf{B_i}b_i u_i + \mathbf{H_i}(x_{1i} - \hat{x}_{1i}) \tag{9}$$

where $\hat{\mathbf{x}}_\mathbf{i}$ is the estimate of $\mathbf{x_i}$ and $\mathbf{H_i}$ is the observer gain matrix denoting as $[\omega_{oi}\alpha_1 \quad \omega_{oi}^2\alpha_2 \quad \omega_{oi}^3\alpha_3]^{\mathrm{T}}$, in which ω_{oi} is the only tuning parameter, also called the bandwidth of the observer and α_k, $k = 1, 2, 3$ are selected such that the characteristic polynomial $s^3 + \alpha_1 s^2 + \alpha_2 s + \alpha_3$ is Hurwitz. For simplicity, here we choose $\alpha_1 = 3, \alpha_2 = 3, \alpha_3 = 1$, which leads to the multiple poles $s = -1$.

Define the estimation error $\tilde{\mathbf{x}}_\mathbf{i} = \mathbf{x_i} - \hat{\mathbf{x}}_\mathbf{i}$. The error dynamics is governed by

$$\dot{\tilde{\mathbf{x}}}_\mathbf{i} = \mathbf{A_i}\tilde{\mathbf{x}}_\mathbf{i} + \mathbf{F_i}(\mathbf{x_i}) - \mathbf{F_i}(\hat{\mathbf{x}}_\mathbf{i}) - \mathbf{H_i}\tilde{x}_{1i} + \mathbf{\Delta_i} \tag{10}$$

Let $\varepsilon_{ki} = \tilde{x}_{ki}/\omega_o^{k-1}$ and $\tilde{F}_{ri} = F_{ri}(x_{1i}, x_{2i}) - F_{ri}(\hat{x}_{1i}, \hat{x}_{2i})$. System (10) can be rewritten as

$$\dot{\varepsilon}_\mathbf{i} = \omega_{oi}\bar{\mathbf{A}}_\mathbf{i}\varepsilon_\mathbf{i} + \mathbf{B_i}\frac{\tilde{F}_{ri}}{\omega_{oi}} + \bar{\mathbf{B}}_\mathbf{i}\frac{h_i}{\omega_{oi}^2} \tag{11}$$

where

$$\varepsilon_\mathbf{i} = \begin{bmatrix} \varepsilon_{1i} \\ \varepsilon_{2i} \\ \varepsilon_{3i} \end{bmatrix}, \bar{\mathbf{A}}_\mathbf{i} = \begin{bmatrix} -\alpha_1 & 1 & 0 \\ -\alpha_2 & 0 & 1 \\ -\alpha_3 & 0 & 0 \end{bmatrix}, \bar{\mathbf{B}}_\mathbf{i} = \begin{bmatrix} 0 \\ 0 \\ 1 \end{bmatrix}.$$

Theorem 1: Under Assumption 1, if the observer is designed as (9), with the proper selection of parameter ω_{oi}, the estimation error of system (10) can asymptotically converge to an arbitrarily small region.

proof: Since $\bar{\mathbf{A}}_\mathbf{i}$ is Hurwitz, there exists a positive definite matrix $\mathbf{P_i}$ satisfying the Lyapunov equation $\bar{\mathbf{A}}_\mathbf{i}^{\mathrm{T}}\mathbf{P_i} + \mathbf{P_i}\bar{\mathbf{A}}_\mathbf{i} = -\mathbf{Q_i}$, where $\mathbf{Q_i}$ is an arbitrarily positive definite matrix. Consider the following Lyapunov function candidate as $V_{1i} = {\varepsilon_\mathrm{i}}^{\mathrm{T}}\mathbf{P_i}\varepsilon_\mathrm{i}$. Taking the derivative of V_{1i} yields

$$\begin{aligned} \dot{V}_{1i} =& \dot{\varepsilon}_\mathrm{i}^{\mathrm{T}}\mathbf{P_i}\varepsilon_\mathrm{i} + {\varepsilon_\mathrm{i}}^{\mathrm{T}}\mathbf{P_i}\dot{\varepsilon}_\mathrm{i} \\ =& (\omega_{oi}{\varepsilon_\mathbf{i}}^{\mathrm{T}}\bar{\mathbf{A}}_\mathbf{i}^{\mathrm{T}} + {\mathbf{B_i}}^{\mathrm{T}}\frac{\tilde{F}_{ri}}{\omega_{oi}} + \bar{\mathbf{B}}_\mathbf{i}^{\mathrm{T}}\frac{h_i}{\omega_{oi}^2})\mathbf{P_i}\varepsilon_\mathrm{i} \\ &+ {\varepsilon_\mathrm{i}}^{\mathrm{T}}\mathbf{P_i}(\omega_{oi}\bar{\mathbf{A}}_\mathbf{i}\varepsilon_\mathbf{i} + \mathbf{B_i}\frac{\tilde{F}_{ri}}{\omega_{oi}} + \bar{\mathbf{B}}_\mathbf{i}\frac{h_i}{\omega_{oi}^2}) \\ =& -\omega_{oi}{\varepsilon_\mathbf{i}}^{\mathrm{T}}\mathbf{Q_i}\varepsilon_\mathbf{i} + 2{\varepsilon_\mathrm{i}}^{\mathrm{T}}\mathbf{P_i}\mathbf{B_i}\frac{\tilde{F}_{ri}}{\omega_{oi}} + 2{\varepsilon_\mathrm{i}}^{\mathrm{T}}\mathbf{P_i}\bar{\mathbf{B}}_\mathbf{i}\frac{h_i}{\omega_{oi}^2}. \end{aligned} \tag{12}$$

Note that

$$\begin{aligned} |\tilde{F}_{ri}| &= -F_{1i}\tilde{x}_{1i} - F_{2i}\tilde{x}_{2i} \\ &\le F_{1i}|\varepsilon_{1i}| + F_{2i}\omega_{oi}|\varepsilon_{2i}| \le (F_{1i} + F_{2i}\omega_{oi})||\varepsilon_\mathbf{i}||. \end{aligned}$$

Then we have

$$\begin{aligned} \dot{V}_{1i} \le& -\omega_{oi}\lambda_{\min}(\mathbf{Q_i})||\varepsilon_\mathbf{i}||^2 + 2(\frac{F_{1i}}{\omega_{oi}} + F_{2i})||\varepsilon_\mathbf{i}||^2||\mathbf{P_i}\mathbf{B_i}|| \\ &+ 2\frac{L_i}{\omega_{oi}^2}||\varepsilon_\mathbf{i}||||\mathbf{P_i}\bar{\mathbf{B}}_\mathbf{i}|| \\ \le& -\Big[\omega_{oi}\lambda_{\min}(\mathbf{Q_i}) - 2(\frac{F_{1i}}{\omega_{oi}} + F_{2i})||\mathbf{P_i}\mathbf{B_i}|| - \frac{L_i}{\omega_{oi}^2}\Big]||\varepsilon_\mathbf{i}||^2 \\ &+ \frac{L_i}{\omega_{oi}^2}||\mathbf{P_i}\bar{\mathbf{B}}_\mathbf{i}||^2 \\ \le& -\mathbf{K_i}V_{1i} + \mathbf{\Xi_i} \end{aligned} \tag{13}$$

where $\lambda_{\min}\{\bullet\}$ and $\lambda_{\max}\{\bullet\}$ denote the minimum and maximum eigenvalues of a symmetric matrix, respectively,

$$\begin{aligned} \mathbf{K_i} =& \frac{\omega_{oi}\lambda_{\min}(\mathbf{Q_i}) - 2(\frac{F_{1i}}{\omega_{oi}} + F_{2i})||\mathbf{P_i}\mathbf{B_i}|| - \frac{L_i}{\omega_{oi}^2}}{\lambda_{\max}(\mathbf{P_i})}, \\ \mathbf{\Xi_i} =& \frac{L_i}{\omega_{oi}^2}||\mathbf{P_i}\bar{\mathbf{B}}_\mathbf{i}||^2. \end{aligned}$$

By using the comparison lemma, it can be inferred from the inequality (13) that V_{1i} is bounded by

$$V_{1i}(t) \le V_{1i}(0)e^{-\mathbf{K_i}t} + \frac{\mathbf{\Xi_i}}{\mathbf{K_i}}(1 - e^{-\mathbf{K_i}t}). \tag{14}$$

It is obvious that by increasing the bandwidth ω_{oi}, the estimation error can be made arbitrarily small.

To guarantee the system stability, the parameter ω_{oi} should satisfy the following condition

$$\lambda_{\min}(\mathbf{Q_i})\omega_{oi}^3 - 2F_{2i}||\mathbf{P_i}\mathbf{B_i}||\omega_{oi}^2 - 2F_{1i}||\mathbf{P_i}\mathbf{B_i}||\omega_{oi} > L_i \tag{15}$$

such that $\mathbf{K_i} > 0$ always hold.

This completes the proof. □

B. ESO-Based SMC design

With the design of ESO (9), not only the unmeasurable state x_{2i} but also the lumped uncertainty D_{di} is estimated, which can be computed as $x_{1i} = \hat{x}_{1i} + \tilde{x}_{1i}$, $x_{2i} = \hat{x}_{2i} + \tilde{x}_{2i}$, $D_{di} = \hat{x}_{3i} + \tilde{x}_{3i}$, where $\tilde{x}_{1i}, \tilde{x}_{2i}$, and $\tilde{x}_{3i}$ are bounded. Assume that the estimation errors are bounded by $|\tilde{x}_{ki}| \le \beta_{ki}$, $k = 1, 2, 3$ after

finite time T. Depending on the estimated state, the sliding surface is designed as

$$s_i = c_i x_{1i} + \hat{x}_{2i} \tag{16}$$

where c_i is the design parameter.

The proposed ESO-based SMC method is designed as

$$u_i = -\frac{1}{b_i}[F_{ri}(x_{1i}, \hat{x}_{2i}) + c_i \hat{x}_{2i} + \hat{x}_{3i} + k_{1i}\text{sign}(s_i) + k_{2i}s_i] \tag{17}$$

where k_{1i} and k_{2i} are control gains to be designed, satisfying the following condition

$$k_{1i} > (F_{1i} + \omega_{oi}^2\alpha_2)\beta_{1i} + c_i\beta_{2i}, k_{2i} > 1. \tag{18}$$

Theorem 2: Considering the case that if the angular rate ω_i is the only available state, under the control law (17), if the observer gain ω_{oi} and switching gain k_i are chosen as (14) and (18), respectively, the tracking error x_{1i} can converge to a small region β_{2i}/c_i in the presence of multiple time-varying disturbances when time tends to infinity.

proof: Consider the Lyapunov function candidate as $V_{2i} = 1/2s_i^2$. Taking the derivative of V_{2i} yields

$$\begin{aligned}\dot{V}_{2i} =& s_i\dot{s}_i \\ =& s_i[c_i\hat{x}_{2i} + c_i\tilde{x}_{2i} + F_{ri}(\hat{x}_{1i}, \hat{x}_{2i}) + b_iu_i \\ &+ \hat{x}_{3i} + \omega_{oi}^2\alpha_2\tilde{x}_{1i}] \\ =& s_i[c_i\tilde{x}_{2i} + F_{ri}(\hat{x}_{1i}, \hat{x}_{2i}) - F_{ri}(x_{1i}, \hat{x}_{2i}) \\ &+ \omega_{oi}^2\alpha_2\tilde{x}_{1i} - k_{1i}\text{sign}(s_i) - k_{2i}s_i] \\ \leq& -2(k_{2i}-1)V_{2i} + \frac{c_i^2|\tilde{x}_{2i}|^2}{2} + \frac{(F_{1i} + \omega_{oi}^2\alpha_2)^2|\tilde{x}_{1i}|^2}{2}.\end{aligned} \tag{19}$$

Similarly with (14), it can be derived from inequality (19) that s_i is bounded if $k_{2i} > 1$ holds.

Considering the Lyapunov function once again, the following inequality can be obtained:

$$\begin{aligned}\dot{V}_{2i} \leq& -\sqrt{2}[k_{1i} - (c_i|\tilde{x}_{2i}| + (F_{1i} + \omega_{oi}^2\alpha_2)|\tilde{x}_{1i}|)]V_{2i}^{\frac{1}{2}} \\ &- 2k_{2i}V_{2i}.\end{aligned} \tag{20}$$

When $t \leq T$, from (19) we have s_i is bounded. When $t > T$, $|\tilde{x}_{1i}| \leq \beta_{1i}$ and $|\tilde{x}_{2i}| \leq \beta_{2i}$ hold. With the condition (18), it can be derived from the inequality (20) that the system states will reach the defined sliding surface (16) in finite time (Remark 2 in [15]).

Once the sliding surface is reached, it implies that

$$c_i x_{1i} + \dot{x}_{1i} - \tilde{x}_{2i} = 0 \tag{21}$$

which can be further transformed into

$$\dot{x}_{1i} \leq -c_i x_{1i} + \beta_{2i}. \tag{22}$$

That is, the tracking error of inertial angular rate is bounded by

$$x_{1i}(t) \leq x_{1i}(0)e^{-c_i t} + \frac{\beta_{2i}}{c_i}(1 - e^{-c_i t}) \tag{23}$$

which means that the state x_{1i} can reach a small region β_{2i}/c_i when t tends to infinity. This completes the proof. □

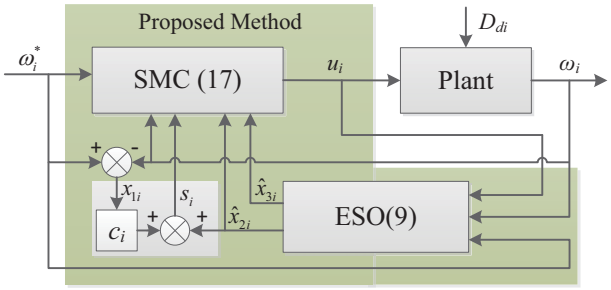

Fig. 2. Block diagram of proposed ESO-based SMC method.

TABLE I
PARAMETERS OF PMDC MOTOR

Parameters	Meaning	Value
U	Rated Voltage	27 V
I_N	Rated Current	2.5 A
R_a	Armature Resistance	10.8Ω
L_a	Armature Inductance	6.5 mH
T_N	Rated Torque	1.0 N·m
k_t	Torque Coefficient	0.4 N·m/A
k_v	Back-EMF Coefficient	0.214 V/(rad/s)
B	Viscous Damping Coefficient	7.4×10^{-5} N· m· s/rad

The block diagram of the proposed ESO-based SMC method is constructed in Fig. 2.

Remark 1: The constraints of the control parameters ω_{oi} and k_i are indicated explicitly as (14) and (17), which provide the basic stability conditions of the closed-loop system. Compared with the traditional SMC, the switching gain k_{1i} of the proposed method is only required to be chosen to restrain the uncertainty caused by states estimation errors x_{1i} and x_{2i} rather than the disturbance D_{di} such that k_{1i} can be designed much smaller than that of general SMC method, which substantially alleviates the chattering problem.

IV. SIMULATION RESULTS

To investigate the efficiency of the proposed output feedback SMC method, simulations on 2-DOF ISP system are performed in comparison with the traditional PI controller. The parameters of the adopted PMDC motors are given in Table I. The nominal inertial matrices of gimbal system are given as

$$J_{AN} = \begin{bmatrix} 0.0435 & 0 & 0 \\ 0 & 0.0652 & 0 \\ 0 & 0 & 0.0435 \end{bmatrix} \text{kg}\cdot\text{m}^2,$$

$$J_{KN} = \begin{bmatrix} 0.0735 & 0 & 0 \\ 0 & 0.0735 & 0 \\ 0 & 0 & 0.0954 \end{bmatrix} \text{kg}\cdot\text{m}^2.$$

Suppose that the angular rate of vehicle motion or frame B is $\mathbf{\Omega_B} = [0, 25\sin 2\pi t, 25\cos 2\pi t]^{\text{T}}$ deg /s. Due to the mass

unbalance, the inertial matrices are set as $J_A = J_{AN} + \Delta J_A$ and $J_K = J_{KN} + \Delta J_K$, where

$$\Delta J_A = \begin{bmatrix} 0.0148 & -0.0329 & -0.0468 \\ -0.0329 & 0.0245 & 0.0375 \\ -0.0468 & 0.0375 & 0.0185 \end{bmatrix} \text{kg} \cdot \text{m}^2,$$

$$\Delta J_K = \begin{bmatrix} 0.0135 & -0.0253 & -0.0235 \\ -0.0253 & 0.0162 & 0.0416 \\ -0.0235 & 0.0416 & 0.0392 \end{bmatrix} \text{kg} \cdot \text{m}^2.$$

The external lumped uncertain torque caused by the optical electronic tracker, cable restraint and wind gust are assumed to be $H_i(\omega_i, t) = (0.02\sin(\pi t) + 0.01)$ N·m.

For the pitch gimbal, the parameters of the proposed method are designed as $\omega_{oq} = 400$, $c_q = 1000$, $k_{1q} = 50$ and $k_{2q} = 30$. The parameters of PI controller are designed as $k_{pq} = 2$ and $k_{iq} = 15$. For the yaw gimbal, the parameters of the proposed method are designed as $\omega_{or} = 450$, $c_r = 1500$, $k_{1r} = 75$ and $k_{2r} = 35$. The parameters of PI controller are designed as $k_{pr} = 5$ and $k_{ir} = 25$. The simulations are carried out under two operation modes, i.e., inertial stabilized mode and target tracking mode [2].

A. Control Performance in Inertial Stabilized Mode

In the inertial stabilized mode, the control task is to keep LOS steady relative to inertial space in the presence of multiple disturbances. The initial values of angular rates q_a and r_a are set as 10 deg/s. The desired angular rate ω_i^* is set as 0. The simulation results in this case are shown in Figs. 3-5.

It can be observed from Figs. 3-4 that both the unknown state x_{2i} and the lumped uncertainty H_{di} are estimated via ESO. As shown in Fig. 3(c) and Fig. 4(c), by choosing relative large values ω_{oi} and c_i, the offsets of the inertial angular rate caused by disturbances are almost entirely removed by the proposed method, while it can only guarantee the system output converge to a wide region by PI controller. Meanwhile, the control chattering existing in the traditional SMC is significantly reduced since the switching gain only needs to be chosen to restrain the uncertainty caused by states estimation errors rather than disturbance itself. From Fig. 5, one can see that the LOS is almost kept still in the steady-state even in the presence of multiple disturbances by the proposed method.

B. Control Performance in Target Tracking Mode

In the target tracking mode, the control task is to keep LOS toward a moving target. The initial values of angular rates q_a and r_a are set as 0. The desired inertial angular rates are set as $\omega_q^* = 10\sin(\pi t)$ deg/s and $\omega_r^* = 10\cos(\pi t)$ deg/s. The simulation result is shown in Fig. 6. For simplicity, we only give the tracking path of LOS in the yaw-pitch plane. It is obvious that the accurate tracking is achieved with the proposed method.

V. Conclusion

The output feedback SMC of ISP system subject to various disturbed phenomena has been investigated in this paper. The ESO depending on the only available signal, i.e., inertial angular rate and the control input has been designed to estimate both the unknown state and lumped uncertainty. The estimates have been brought into the design of output feedback SMC and the switching gain can be chosen much smaller such that chattering problem is significantly alleviated. Theoretical analysis has verified that the output can converge to an arbitrarily small region. Comparative simulations with traditional PI control have been performed to show the effectiveness of the proposed method in two typical operation mode.

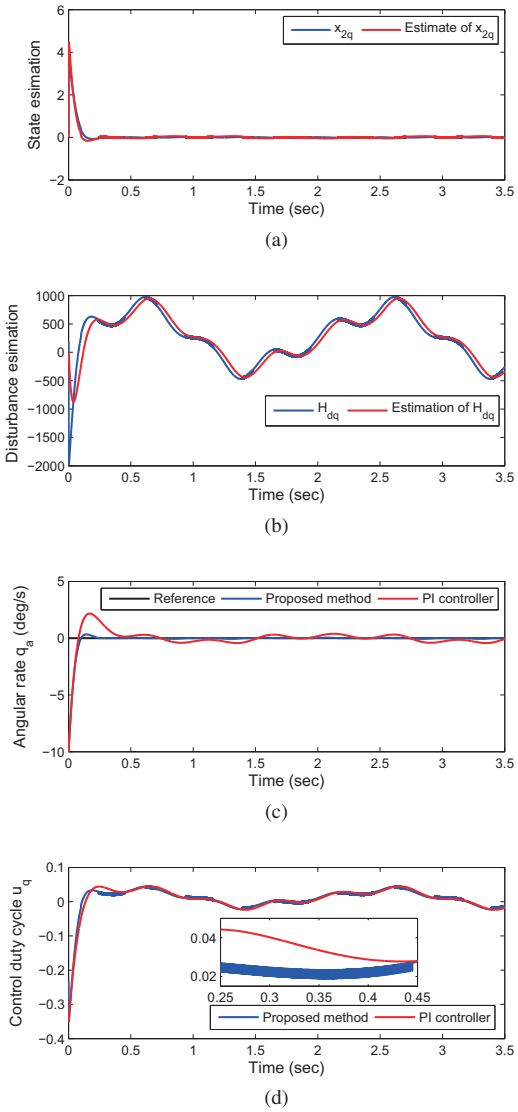

Fig. 3. Response curves of pitch gimbal system: (a) Estimation of state x_{2q}, (b) Estimation of uncertainty D_{dq}, (c) Angular rate q_a, and (d) Control duty cycle u_q.

Acknowledgment

The authors would like to thank International Science & Technology Cooperation Program of China (2015DFA10490) and National Natural Science Foundation of China (61573099) and the Innovate Foundation for Graduate Student of JiangSu Province (KYLX15_0213).

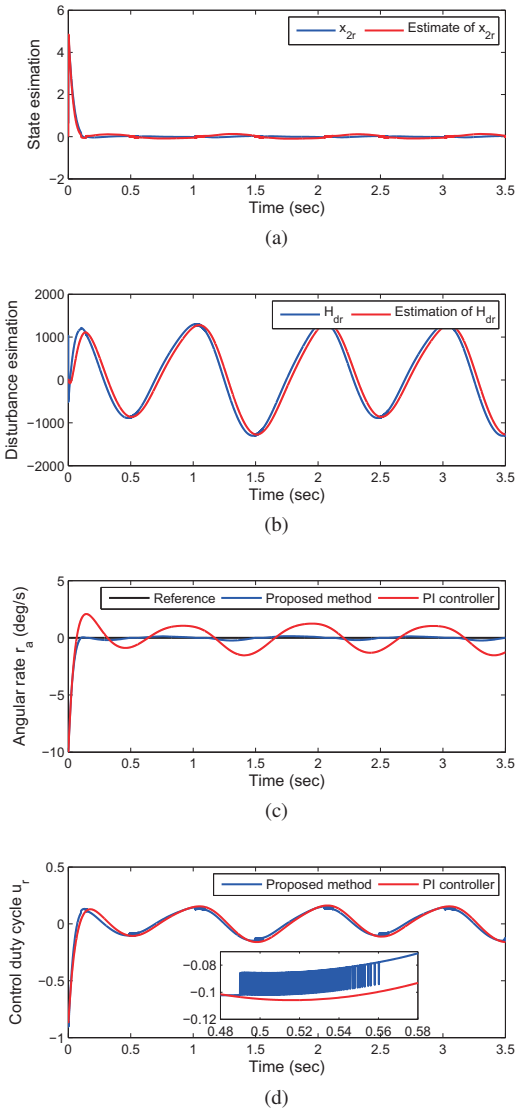

Fig. 4. Response curves of yaw gimbal system: (a) Estimation of state x_{2r}, (b) Estimation of uncertainty D_{dr}, (c) Angular rate r_a, and (d) Control duty cycle u_r.

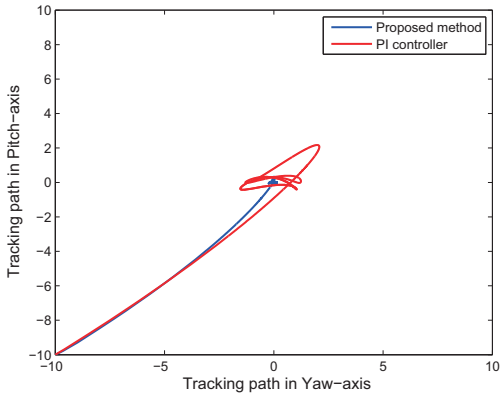

Fig. 5. Tracking path of LOS in the yaw-pitch plane under inertial stabilized mode.

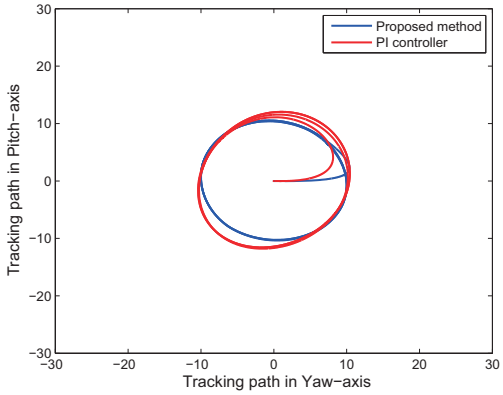

Fig. 6. Tracking path of LOS in the yaw-pitch plane under target tracking mode.

REFERENCES

[1] J. M. Hilkert, "Inertially stabilized platform technology concepts and principles," *IEEE Control System Magzine*, 28(1), 26-46, 2008.

[2] Z. Hurák and M. Řezáč, "Image-based pointing and tracking for inertially stabilized airborne camera platform," *IEEE Transactions on Control Systems Technology*, 20(5), 1146-1159, 2012.

[3] M. Abdo, A. Vali, A. Toloei, and M. Arvan, "Stabilization loop of a two axes gimbal system using self-tuning PID type fuzzy controller," *ISA Transactions*, 53(2), 591-602, 2014.

[4] M. Řezáč and Z. Hurák, "Structured MIMO H∞ design for dual-stage inertial stabilization: case study for HIFOO and hinfstruct solvers," *Mechatronics*, 23(8), 1084-1093, 2013.

[5] X. Y. Zhou, H. Y. Zhang, and R. X. Yu, "Decoupling control for two-axis inertially stabilized platform based on an inverse system and internal model control," *Mechatronics*, 24(8), 1203-1213, 2014.

[6] J. Fang, R. Yin, and X. Lei, "An adaptive decoupling control for three-axis gyro stabilized platform based on neural networks," *Mechatronics*, 27, 38-46, 2015.

[7] J. Yang, S. Li, and X. Yu, "Sliding-mode control for systems with mismatched uncertainties via a disturbance observer," *IEEE Transactions on Industrial Electronics*, 60(1), 160-169, 2013.

[8] J. Han, "From PID to active disturbance rejection control," *IEEE transactions on Industrial Electronics*, 56(3), 900-906, 2009.

[9] Q. Zheng, L. Gao, and Z. Gao, "On stability analysis of active disturbance rejection control for nonlinear time-varying plants with unknown dynamics," *In Proceedings of IEEE Conference on Decision and Control*, 2007, 3501-3506.

[10] J. Yao, Z. Jiao, and D. Ma, "Adaptive robust control of dc motors with extended state observer," *IEEE Transactions on Industrial Electronics*, 55(7), 3630-3637, 2014.

[11] S. Li, J. Yang, W.-H Chen, and X. Chen, "Generalized extended state observer based control for systems with mismatched uncertainties," *IEEE Transactions on Industrial Electronics*, 59(12), 4792-4802, 2012.

[12] J. Yao, Z. Jiao, and D. Ma, "Extended-state-observer-based output feedback nonlinear robust control of hydraulic systems with backstepping," *IEEE Transactions on Industrial Electronics*, 61(11), 6285-6293, 2014.

[13] Q. Guo, Y. Zhang, B. G. Celler, and W. S. Steven, "Backstepping Control of Electro-Hydraulic System Based on Extended-State-Observer With Plant Dynamics Largely Unknown," *IEEE Transactions on Industrial Electronics*, 63(11), 6909-6920, 2016.

[14] B. Ekstrand, "Equations of motion for a two-axes gimbal system," *IEEE Transactions on Aerospace and Electrononic System*, 37(3), 1083-1091, 2001.

[15] S. Yu, X. Yu, B. Shirinzadeh, and Z. Man, "Continuous finite-time control for robotic manipulators with terminal sliding mode," *Automatica*, 41(11), 1957-1964, 2005.